# RETRIEVAL OF CLOUD GEOMETRICAL PARAMETERS USING REMOTE SENSING DATA

Makoto Kuji[*a] and Teruyuki Nakajima[b]

[a]Dept. of Computer and Information Sciences, Nara Women's Univ., Japan

[b]Center for Climate System Research, Univ. of Tokyo, Japan

## ABSTRACT

It is of great interest to investigate the properties on the cloud optical, microphysical, and geometrical parameters, in particular, of low-level marine clouds which have crucial influence on the global climate system. Top height, bottom height, and geometrical thickness of cloud layer are considered here as cloud geometrical parameters. These parameters are very important, because top and bottom heights are the factors which govern the strength of greenhouse effect through the thermal radiation from / to cloud layer, whereas the geometrical thickness is the key parameter for the estimation of gaseous absorption in a cloud layer where multiple scattering process dominates.

In this study, an algorithm was developed to retrieve simultaneously cloud optical thickness, effective particle radius, top height, and geometrical thickness of cloud layer from the spectral information of visible, near infrared, thermal infrared, and oxygen A band channels. This algorithm was applied to the First ISCCP Regional Experiment (FIRE, conducted in 1987) airborne data which included the relevant four channels and targeted at the low-level marine clouds off the coast of California in summer. The retrieved results seems to be comparable to the in situ microphysical observation. But, for the cloud geometrical parameters (top and bottom heights), compared to lidar observation, variance of the retrieved cloud bottom height is rather large for multilayered cloud system in particular.

The other data sets, recently observed in airborne and spaceborne measurement, will further be analyzed, so as to confirm the algorithm's utility and check the limitation on a regional and global scale, respectively. The algorithm will be applied to the Global Imager (GLI) spaceborne data set to make global cloud products. The GLI will be onboard with Advanced Earth Observing Satellite-II (ADEOS-II) satellite which will be launched in 2002 by National Space Development Agency of Japan (NASDA).

[*]Correspondence author address: Makoto Kuji, Dept. of Computer and Information Sciences, Nara Women's Univ., Japan, 630-8506; e-mail: makato@ics.nara-wu.ac.jp.

## 1. INTRODUCTION

Global observations by satellites reveal the radiation budget at top of the atmosphere of the earth. But an estimation of surface radiation budget has not been clear yet. It is said that the uncertainty of cloud base height is one of the sources of this vagueness, as well as water vapour anomalous absorption.

Investigation using oxygen absorption spectral bands has chronologically long history. Yamamoto and Wark (1961) literally suggested that the utility of oxygen A band information to estimate the cloud top height rather than the carbon dioxide due to its mixing of the absorption lines with the ones of water vapour. Saiedy et al. (1967) studied that the cloud top determination with hand-held spectrograph-camera observation by Gemini-5 astronauts and suggested that the correction method for the photon penetration with the solar zenith, viewing and azimuthal angles. Curran et al. (1981) showed that the multichannel scanning radiometer which had the two channel in oxygen A band, had the utility of cloud top altitude detection. Wu (1985) had investigated that the cloud top height retrieval using the spectral observation around the oxygen A band. His approach was called as the radiance ratio method and he discussed the correction of photon penetration effect had to be taken into consideration for his method. Fischer and Grassl (1991a) and Fischer et al. (1991b) made the more detailed analysis for cloud top estimation using the oxygen A band by validating the synchronized Lidar observation. Hayasaka et al. (1995), on the

other hand, developed the retrieval algorithm of cloud geometrical thickness from a measured liquid water path and equivalent width of 0.94 µm water vapor absorption band and applied to aircraft observations to retrieve the geometrical thickness, and the results were smaller than those observed by eye. Asano et al. (1995) showed the retrieval algorithm of the cloud optical, microphysical, and geometrical parameters simultaneously using the aircraft flux observations. Nakajima et al. (1998) recently showed the sensitivity estimation of the oxygen A band radiance to be observed from space to the geometrical parameters for preparation of 2002 launch of Advanced Earth Observing Satellite-II (ADEOS-II) Global Imager (GLI).

In this study, an algorithm was developed to retrieve the cloud optical thickness, effective particle radius, top height, and geometrical thickness of cloud layer simultaneously using the four spectral information such as the visible, near infrared, thermal infrared, and oxygen A band. This algorithm was applied to the airborne observation data and the retrieved results were compared to in situ ground-based and airborne observations.

## 2. DESCRIPTION OF OBSERVATION AND DATA

The cloud features, the airborne observation and the sensor spectral specification concerned to our analyses are described in this section.

There extends marine stratocumulus cloud system over the east Pacific Ocean in summer. Targeting this cloud system, First International Satellite Cloud Climate Project (ISCCP) Regional Experiment (FIRE) Marine Stratocumulus - Intensive Field Observation (MS-IFO) was conducted (Albrecht et al. 1988).

The cloud system we analyzed were also described in Nakajima et al. (1991). There existed the typical marine stratocumulus cloud system with about 1 km in cloud top height and several hundred meters in geometrical thickness.

Multichannel Cloud Radiometer (MCR) onboard NASA ER-2 aircraft carried out the radiative observation above the cloud layer. Spectral specification of MCR is briefly shown in Table 1. MCR has seven channels from visible to thermal infrared spectral region. The visible (ch.1) and two oxygen A band (ch.2 and ch.3) have around 1 nm in Full Width Half Maximum (FWHM), while near

infrared (ch.4, ch.5, and ch.6) have several to several tens nm, and thermal infrared (ch.7) 900 nm, respectively. The ch.2 and ch.3 locate at R- and P-branch of the oxygen A band, respectively.

**Table 1.** Spectral specification of MCR. FWHM means the Full Width Half Maximum of the response function.

| channel number | wavelength (µm) | FWHM (nm) | comment |
|---|---|---|---|
| 1 | 0.754 | 1.08 | |
| 2 | 0.761 | 1.21 | R-branch |
| 3 | 0.764 | 1.12 | P-branch |
| 4 | 1.38 | 8.8 | Water Vapor |
| 5 | 1.65 | 54 | |
| 6 | 2.16 | 89.4 | |
| 7 | 10.8 | 900 | |

The ER-2 carried out fifteen flights in total on July 10 1987. The analyzed MCR scan data in this study is nadir pixels of the flight number 04. There are around 2463 pixels in flight direction. The time when observation was carried out was around 1645 in Universal Time Coordinated (UTC). That corresponds to 0945 in the morning of the local time (Pacific Daylight Time: PDT=UTC-0700).

C-131A University Washington also flew, mounted the PMS probes to observe the cloud microphysical quantities such as the effective particle radius and the Johnson-Williams hot wire probe to observe liquid water content in and around the marine stratocumulus cloud layer.

## 3. METHODOLOGY

The retrieval algorithm and analysis flow are described in this section.

### 3.1 *Principle of Retrieval Algorithm*

Oxygen molecules mixes well in the earth atmosphere with constant mixing ratio. That is why oxygen A band observations from airborne platform have been used mainly to retrieve the cloud top height (or pressure) only, considering of the absorption by oxygen molecules above the cloud top.

In that algorithm, photon penetration into the cloud layer is considered as a retrieval error to be corrected. We could utilize this penetration effect, on the other hand, to retrieve the cloud geometrical properties. That is, photon path length distributions with multiple scattering process in the cloud layer depend upon both the cloud liquid water path and the liquid water content. If the liquid water path is estimated from other method, then the cloud geometrical thickness is determined in turn.

Actually, oxygen A band (rather P-branch than R-branch) spectral radiance to be observed by the high altitude airborne platform is equally sensitive to both the cloud top height and geometrical thickness, for the optically thick cloud system like this marine stratocumulus field. In the cloud layer, the multiple scattering process is dominant, and then photon path length distribution depends upon the liquid water content. Thermal radiance, on the other hand, is mainly sensitive to the cloud top temperature for optically thick clouds. That's why multichannel information makes us to retrieve the cloud geometrical top height and geometrical thickness simultaneously.

### 3.2 *Algorithm Flow*

Figure 1 illustrates the algorithm flow chart. The four spectral channels are necessary to retrieve the cloud optical thickness, effective particle radius, cloud top height, and geometrical thickness of cloud layer. Plane-parallel model atmosphere is assumed to make lookup tables by the theoretical calculation. Supplementary data are necessary to make the lookup tables, such as the total ozone column amount (O3), the relative humidity profile (RH), the temperature profile (TZ), and the surface pressure (PS).
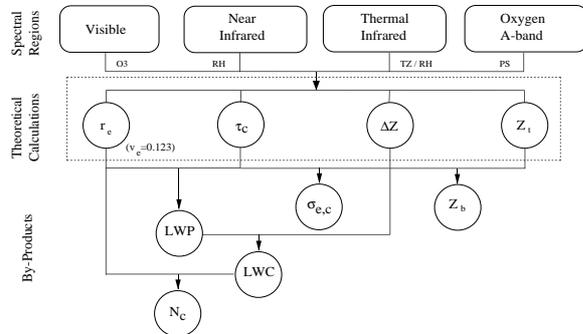


**Figure 1.** Algorithm flow chart. The cloud particle size distribution is assumed as the volume log-normal distribution and the effective variance is also assumed as 0.123.

Cloud optical thickness $\tau_c$ and effective droplet radius $r_e$ are essentially retrieved using visible and near infrared spectral radiance information, and also liquid water path (LWP) as a by-product from the relationship (Stephens 1990):

$$LWP = \frac{2}{3}\tau_c \cdot r_e \cdot \rho_w, \qquad (1)$$

where $\rho_w$ is the density of water.

Top height $z_t$ and the geometrical thickness $\Delta z$ of a cloud layer are also retrieved using the retrieved optical thickness and effective particle radius at the previous step. The cloud bottom height $z_b$ is derived from the cloud top height and the cloud geometrical thickness as follows:

$$z_b = z_t - \Delta z. \qquad (2)$$

The liquid water content (LWC) is derived from the liquid water path and cloud geometrical thickness as follows:

$$LWC = \frac{LWP}{\Delta z}. \qquad (3)$$

The cloud particle size distribution $n(r)$ is assumed as log-normal distribution function:

$$n(r) = \frac{N}{\sqrt{2\pi}\sigma r}\exp\left[-\frac{\left(\ln r - \ln r_0\right)^2}{2\sigma^2}\right], \quad (4)$$

where $r_0$ is the mode radius and $\sigma$ is the standard deviation of the distribution function. $N$ is the total number of cloud particles. The volume $V$ is then defined as

$$V = \int \frac{4\pi}{3}r^3 n(r)dr,$$

$$= N \cdot \frac{4\pi}{3}r_e^3 \exp\left(-3\sigma^2\right). \quad (5)$$

The number concentration $N_c$ is derived from

the liquid water content and effective particle radius assuming the volume spectrum:

$$N_c = \frac{LWC}{\rho_w \cdot \left(\dfrac{V}{N}\right)},$$

$$= \frac{LWC}{\rho_w \cdot \dfrac{4\pi}{3} r_e^3 \exp\left(-3\sigma^2\right)}, \quad (6)$$

where $\sigma$ is assumed as 0.34 and Eq. (5) is used in this calculation.

The volume extinction coefficient of cloud $\sigma_{e,c}$ is derived from the optical thickness and the geometrical thickness of a cloud layer:

$$\sigma_{e,c} = \frac{\tau_c}{\Delta z}. \quad (7)$$

### 3.3 *Retrieval Flow*

Figure 2 illustrates the retrieval flow chart. This is the iterative retrieval. Firstly, scan geometry such as the solar zenith angle, sensor zenith angle, and sun-sensor relative azimuthal angle is setup in the model atmosphere. Secondly, initial values of the optical thickness of cloud, the effective particle radius, cloud top height, and cloud geometrical thickness are assumed. And then, the optical thickness and the effective particle radius of cloud are simultaneously determined from the visible and the near infrared observed radiance with the lookup table calculation using the cloud top height and cloud geometrical thickness assumed at previous step. After that, the cloud top height and the cloud geometrical thickness are simultaneously determined from the thermal and the oxygen A band (P-branch) observed radiance with the lookup table values using the optical thickness of cloud and the effective particle radius determined at previous step. The determined four parameters such as the optical thickness of cloud, the effective particle radius, the cloud top height, and the cloud geometrical thickness, are thus compared to those of previous values. If the difference between the

previous values and the result ones are within the prescribed criterion, then the four parameters are retrieved, else another iteration should be carried out.
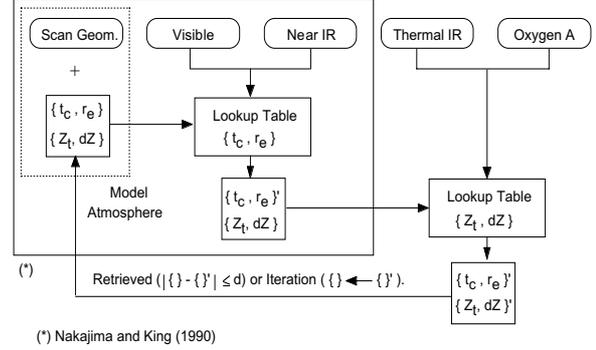


**Figure 2.** Retrieval flow chart. The portion surrounded with the large rectangle corresponds to the retrieval procedure in Nakajima and King (1990). The lookup table in this flow chart is specified with seven-dimensional parameters in single table, such as the scan geometry (solar zenith, sensor zenith, and sun-sensor relative azimuth), the optical thickness, the effective particle radius, cloud top height, and geometrical thickness.

## 4. RESULTS

From the retrieval algorithm as described in previous section, the following four geophysical parameters of cloud layer such as cloud optical thickness, effective particle radius, cloud top height, and cloud geometrical thickness are directly retrieved. The by-products such as the geometrical thickness of cloud layer, liquid water path, liquid water content, and particle number concentration are derived from the above parameters. Those parameters are analyzed for the data set along the MCR flight line.

Figure 3 illustrates the retrieved results of (a) optical thickness of cloud, (b) effective particle radius, and (c) liquid water path, respectively. The liquid water path is derived from the optical thickness of cloud and effective particle radius using Eq. (1).
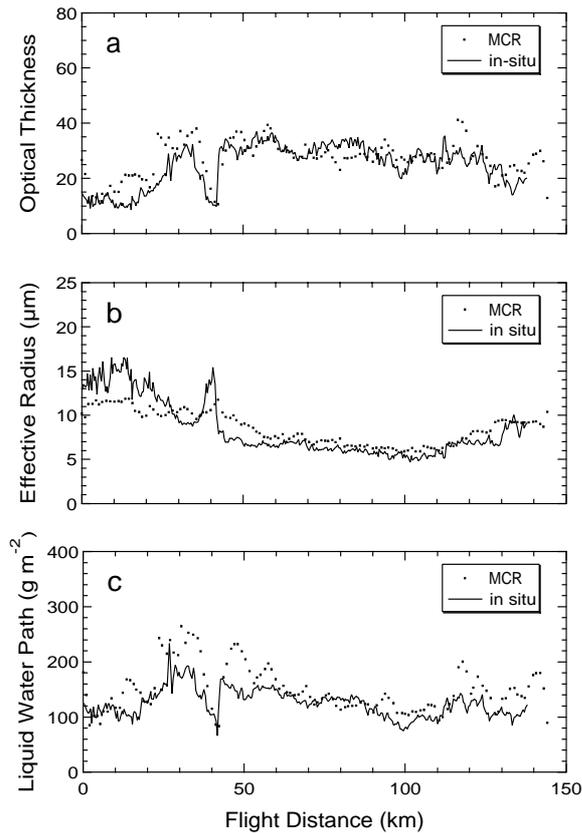
**Figure. 3.** The retrieved results of the cloud parameters along the ER-2 flight; (a) optical thickness of cloud, (b) effective particle radius, and (c) liquid water path. These results are only for the nadir pixels of MCR on ER-2 with flight number 04 on 10 July 1987. The dots are the results from the MCR observation and the solid line is the result from the in situ observation in panels (a), (b) and (c). The liquid water path is a by-product.

The results of the in situ observation are plotted in solid lines as well as the retrieved results from MCR observation in dots. It can be seen that spatial correspondence is good for all three parameters. From Fig. 3b, it can be seen that some discrepancy exists 0-50 km at the flight distance for the effective particle radius due to the drizzle mode particles (Nakajima and King 1990). The in situ effective particle radius is observed with PMS Probe onboard the C-131A aircraft flowing in the middle level of the cloud layer. The in situ liquid water path is derived from the in situ liquid water content observation with the Johnson-Williams hot wire probe with the fixed cloud geometrical thickness (400 m) assumed and then in situ cloud optical thickness is derived from the liquid water path and the in situ effective particle radius (Nakajima and King 1990).

Figure 4 illustrates the retrieved results of (d) top height, (e) geometrical thickness, and (f) bottom height of cloud layer. The bottom height is derived from the cloud top height and the geometrical thickness using Eq. (2). From Figure 4d, it can be seen that the retrieved cloud top height varies from 0.8-1.1 km and two sharp peaks exist at around 70 and 130 km in MCR flight distance. The geometrical thickness of cloud layer, on the other hand, varies from 0.1-0.9 km correlated to the cloud top height. As a result of those two parameters, the cloud bottom height is derived and varies from 0.2-0.9 km which has rather larger variability than the cloud top height. The in situ aircraft observation indicates the cloud geometrical thickness and the cloud bottom height are comparable to this retrieved results from MCR observation (top: 930m; bottom: 490m; Nakajima et al. 1991).
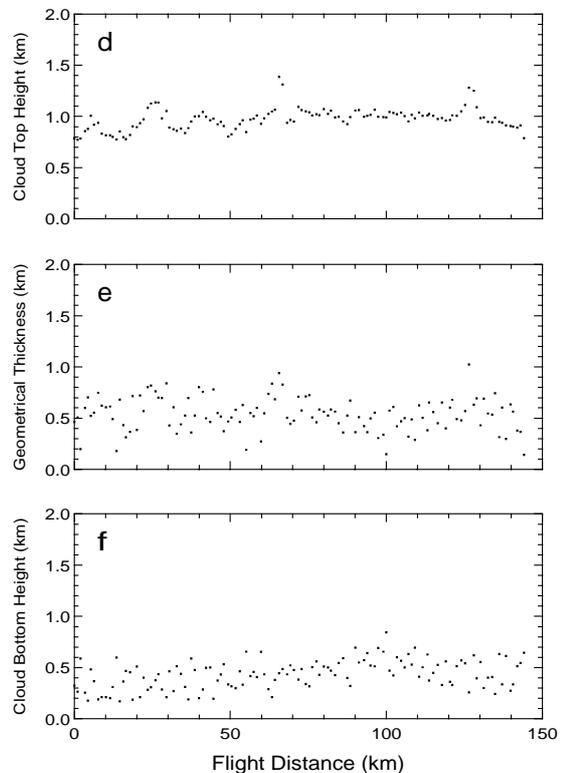


**Figure 4.** As in Fig. 3, except for (d) cloud top height, (e) cloud geometrical thickness, and (f) cloud bottom height. The cloud bottom height is a by-product.

Figure 5 illustrates the results of the py-products for (g) liquid water content, (h) particle number concentration, and (i) extinction coefficient. The liquid water content is derived from the liquid

water path and the geometrical thickness of cloud layer using Eq. (3). The particle number concentration is derived from the liquid water content and the effective particle radius using Eq. (6) assumed the given standard deviation of the size distribution function in Eq. (4). The extinction coefficient is derived from the optical thickness and the geometrical thickness using Eq. (7). From Fig. 5g, it can be seen that the derived liquid water content is systematically smaller than the in situ observation with the Johnson-Williams hot wire probe. This discrepancy is larger at 50-150 km (non drizzle mode region) in the MCR flight distance and attributed to the larger retrieved values in the cloud geometrical thickness. The variation of the liquid water content is good in spite of those biases. The particle number concentration is derived as the typical values of the marine stratocumulus by the order of a few hundred $cm^{-3}$ (Fig. 5h). From Figs. 3c, 5g, and 5h, it can be seen that at 0-50 km region of the MCR flight distance, the retrieved liquid water path and liquid water content are almost same order as those at the other region although the particle number concentration of that region is smaller than that of 50-150 km region. This feature indicates that there exist larger size droplets at the 0-50 km region than at the other region (Nakajima et al. 1991).
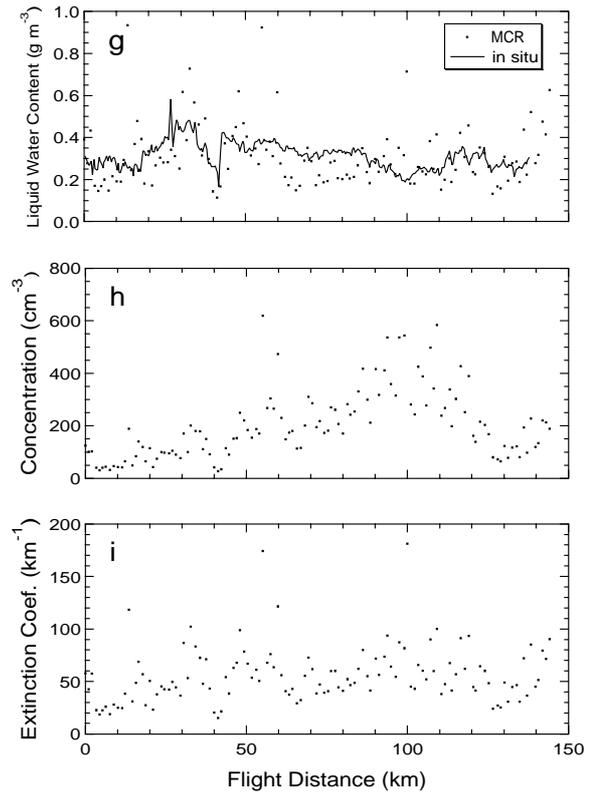


**Figure 5.** As in Fig. 3, except for (g) liquid water content, (h) number concentration of cloud particles, and (i) extinction coefficient of a cloud layer. The dots are the results from the MCR observation and the solid line is the results from the in situ observation in the panel (g). The liquid water content, number concentration, and extinction coefficient, are by-products.

## 5. DISCUSSION

The retrieved results are discussed in this section.

### 5.1 *Reanalysis of Visible - Near Infrared Retrieval and its Validation*

The retrieval of the optical thickness of cloud and the effective particle radius from the visible and near infrared spectral information has been already investigated using the same MCR data set as this study (Nakajima and King 1990; Nakajiama et al. 1991). The retrieved results of the effective droplet radius in their studies were overestimated from the in situ aircraft observation even after the correction from the droplet profile within the cloud layer. The cause of this discrepancy are supposed

to the following two points: One is the treatment of the filter response function for the near infrared channel (ch.6). Another is the treatment of the gaseous absorption influence. The first point to be revised is that only the center of the response function was taken into consideration. In this study, the other calculations were executed which took the filter response function into account. The lookup table is not largely different between the one point (only center) calculations and the filter weighted calculations. This indicates the filter response is not the very cause for above discrepancy. The second point to be revised is that the estimation of the gaseous absorption is based upon the LOWTRAN 5 model. It was indicated that the LOWTRAN 7 model is better for the effective droplet radius retrieval rather than LOWTRAN 5 model (Taylor 1992). The retrieved effective particle radius shows good coincidence in the variation and the magnitude to the in situ aircraft observation within the cloud layer. According to those results, the discrepancy in the effective droplet radius retrieval is almost resolved by using the LOWTRAN 7 model gaseous absorption and the retrieved effective droplet radius is reliable with this validation.

### 5.2 *Validation of Cloud Geometrical Parameters*

Next, in order to make validation of cloud top and bottom heights, the retrieved values are compared to the LIDAR observation. This LIDAR and MCR were mounted on the ER-2 aircraft simultaneously.

Figure 6 illustrates the cloud top and bottom heights retrieved with MCR data. It is identical to a combination of Fig. 5a and Fig. 5c. Figure 7 illustrates, on the other hand, the results of the LIDAR observation of the same ER-2 flight. This indicates that the cloud system showed a two-layered cloud system; one locates from 12 to 14 km height and the other does around 1 km height. It is interpreted that higher-level cloud is cirrus and lower-level one is summer stratus or marine stratocumulus.
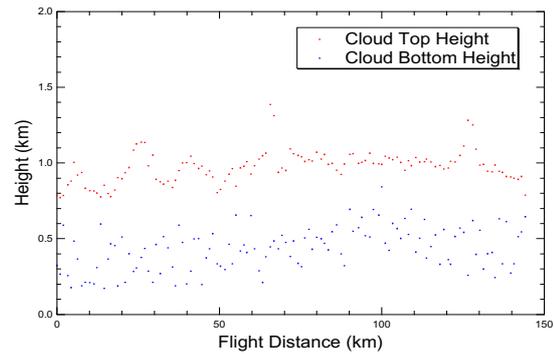


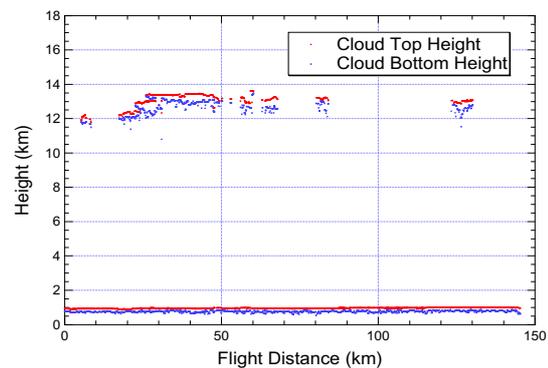**Figure 6.** Retrieved cloud top and bottom heights using MCR data.



**Figure 7.** Results of cloud top and bottom heights with LIDAR observation data for July 10, 1987, flight number 4. The red and blue dots are cloud top and bottom heights, respectively.

The retrieved results represent the feature of the combined higher- and lower-cloud system, since the four-channel algorithm in this study assumes the single cloud layer and mainly targets lower-level cloud system. Figure 8 shows the lower-level cloud layers of Fig. 7 in detail. Comparing Fig. 6 to Fig. 8, it turns out that the retrieved cloud top height is same with the lower-level cloud top height estimated with LIDAR on average. But, MCR-retrieved cloud top height has some spike-like feature in a few parts, which is expected to be due to the higher-level cloud contamination. In terms of the cloud bottom height, however, it turns out that there is great difference each other. This discrepancy may be also attributed to the cirrus contami-
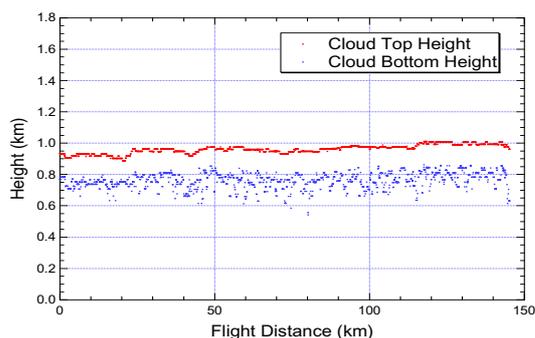
nation at this stage.



**Figure 8.** As in Fig. 7, except for only lower-level clouds.

### 5.3 *Validation of Cloud Microphysical Parameters*

The in situ liquid water content is observed with Johnson-Williams hot wire probe. There are some biases in the liquid water content between the retrieved results and in situ observations due to the discrepancy in the geometrical thickness of cloud layer, too.

## 6. SUMMARY

The airborne radiative observation data were analyzed to retrieve the marine stratocumulus cloud parameters. The retrieved results were partly consistent with in situ airborne observation. As a result of this analysis, it turns out that the combination of the four spectral information such as visible, oxygen A band, near infrared, and thermal infrared has possibility to retrieve cloud optical thickness, effective particle radius, cloud top height, and cloud geometrical thickness simultaneously. The liquid water path, cloud bottom height, liquid water content, number concentration, and extinction coefficient, are derived as by-products as well. It is necessary to analyze another data set and validate the retrieved results for cloud top and bottom height in particular. It is also required to carry out observation for the cloud top and bottom height to validate the retrieved results. If this algorithm will be applied to the global data set such as GLI / ADEOS-II, it is expected to obtain information of the cloud geometrical properties in global scale.

## REFERENCES

Albrecht, B. A., D. A. Randall, and S. Nicholls, 1988: Observations of marine stratocumulus clouds during FIRE. *Bull. Amer. Meteor. Soc.* **69,** 618-626.

Asano, S., M. Shiobara, and A. Uchiyama, 1995: Estimation of Cloud Physical Parameters from Airborne Solar Spectral Reflectance Measurements for Stratocumulus Clouds. *J. Atmos. Sci.,* **52,** 3556-3576.

Blaskovic, M., R. Davies, and J. B. Snider, 1991: Diurnal variation of marine stratocumulus over San Nicolas Island during July 1987. *Mon. Wea. Rev.,* **119,** 1469-1478.

Curran, R. J., H. L. Kyle, L. R. Blaine, J. Smith, and T. D. Clem, 1981: Multichannel scanning radiometer for remote sensing cloud physical parameters. *Rev. Sci. Instrm.,* **52,** 1546-1555.

Fischer, J., and H. Grassl, 1991: Detection of Cloud-Top Height from Backscattered Radiances within the Oxygen A Band. Part 1: Theoretical Study. *J. Appl. Meteor.,* **30,** 1245-1259.

Fischer, J., W. Cordes, A. Schimits-Peiffer, W. Renger, and P. Moerl, 1991: Detection of Cloud-Top Height from Backscattered Radiances within the Oxygen A Band. Part 2: Measurements. *J. Appl. Meteor.,* **30,** 1260-1267.

Hayasaka, T., T. Nakajima, Y. Fujiyoshi, Y. Ishizaka, T. Takeda, and M. Tanaka, 1995: Geometrical Thickness, Liquid Water Content, and Radiative Properties of Stratocumulus Clouds over the Western North Pacific. *J. Appl. Meteor.,* **34,** 460-470.

Nakajima, T., and M. D. King, 1990: Determination of the optical thickness and effective particle radius of clouds from reflected solar radiation measurements. Part I: Theory. *J. Atmos. Sci.,* **47,** 1878-1893.

Nakajima, T., M. D. King, J. D. Spinhirne, and L. F. Radke, 1991: Determination of the optical thickness and effective particle radius of clouds from reflected solar radiation measurements. Part II: Marine Stratocumulus Observations. *J. Atmos. Sci.,* **48,** 728-750.

Nakajima, T. Y., T. Nakajima, M. Nakajima, H. Fukushima, M. Kuji, A. Uchiyama, and M. Kishino, 1998: The optimization of the Advanced Earth Observing Satellite II Global Imager channels by use of radiative transfer calculations. *Appl. Opt.,* **37,** 3149-3163.

Saiedy, F., H. Jacobowitz, and D. Q. Wark, 1967: On Cloud-Top Determination from Gemini-5. *J. Atmos. Sci.,* **35,** 63-69.

Stephens, G. L., 1978: Radiation profiles in extended water clouds II: Parameterization schemes. *J. Atmos. Sci.,* **35,** 2123-2132.

Taylor, J. P., 1992: Sensitivity of remotely sensed effective radius of cloud droplets to changes in LOWTRAN version. *J. Atmos. Sci.,* **49,** 2564-2569.

Wu, M. -L. C., 1985: Remote Sensing of Cloud-Top Pressure Using Reflected Solar Radiation in the Oxygen A-Band. *J. Climate Appl. Meteor.,* **24,** 539-546.

Yamamoto, G., and D. Q. Wark, 1961: Discussion of the Letter by R. A. Hanel, 'Determination of Cloud Altitude from a Satellite'. *J. Geophys. Res.,* **66,** 3596.